Available online at www.sciencedirect.com

ScienceDirect

IFAC Papers Online CONFERENCE PAPER ARCHIVE

IFAC PapersOnLine 50-1 (2017) 2965–2970

Set-point Control of Motion Systems with Uncertain Set-valued Stribeck Friction ⋆

Ruud Beerens * **Henk Nijmeijer** * **Maurice Heemels** *
Nathan van de Wouw *

* *Department of Mechanical Engineering, Eindhoven University of Technology, P.O. Box 513, 5600 MB Eindhoven, The Netherlands (e-mail:{r.beerens; h.nijmeijer; w.p.m.h.heemels; n.v.d.wouw}@tue.nl)*

Abstract: In this paper, we present a control architecture for the set-point stabilization of motion systems subject to set-valued friction, including a velocity-weakening (Stribeck) effect. The proposed controller consists of a switching PID term and a term that robustly compensates for the Stribeck effect. It is shown that the controller asymptotically stabilizes the set-point, and a particular design of the integrator part of the PID controller term allows for faster convergence when overshoot occurs, compared to a conventional integrator. Moreover, this controller is shown to be robust for unknown static friction, and an uncertain contribution of the Stribeck effect. The working principle of the controller is illustrated by means of a numerical example.

Keywords: Discontinuous control, Output feedback control, Asymptotic stabilization

1. INTRODUCTION

In this paper, we present a new control method for set-point stabilization of motion systems subject to static friction and a velocity-weakening (i.e., Stribeck) effect. It is well known that friction is a performance limiting factor in high-precision positioning systems. Indeed, the presence of friction can induce non-zero steady state position errors, friction-induced limit cycling (*hunting*) and large settling times (Armstrong-Hélouvry et al. [1994]). Moreover, friction-induced stick-slip vibrations lead to kinetic energy dissipation, noise, excessive wear, and premature failure of machine parts (Armstrong-Hélouvry et al. [1994]). Throughout the literature, many different approaches have been presented that attempt to compensate for (or reduce) the effects of friction in order to achieve high precision positioning and/or superior trajectory tracking. An obvious solution is to alter the mechatronic design of the positioning equipment early in the development phase such that friction is minimized (by, e.g., the use of high-end bearings, magnetic stages or piezo-electric actuation). Such low-friction mechatronic designs are, however, typically expensive. Therefore, it is appealing to deal with friction via smart (and cheap) control software, where one may try to compensate for friction, or to design control algorithms that achieve high positioning accuracy despite apparent frictional effects.

Two classes of control architectures that deal with friction can be distinguished, namely friction-compensation techniques, and non-compensation-based techniques. The former relies on the compensation of friction by means of including a (parametric) friction model either in a feedback or a feedforward loop in the control system, see e.g., Armstrong-Hélouvry et al. [1994], Putra et al. [2007], Makkar et al. [2007], Olsson and Astrom [1996], Márton and Lantos [2009], Freidovich et al. [2010], Rijlaarsdam et al. [2012]. A general drawback of these friction compensation techniques is the difficulty of developing an accurate friction model with limited complexity, suitable for online control implementation. Moreover, as modeling errors are inevitable, positioning accuracy is compromised due to over- or undercompensation of the friction, see Putra et al. [2007]. In addition, the friction characteristic may change due to changing operating conditions (e.g., temperature or wear), which may increase the friction model mismatch. To overcome the latter problem, adaptive control, see e.g., Amthor et al. [2010], Na et al. [2014], Panteley et al. [1998], may introduce a certain level of robustness against changing or uncertain friction conditions by a continuous online update of the parameters of the friction model used in the control law. Modeling errors, however, still remain and deteriorate the positioning performance.

An advantage of non-compensation-based schemes is that they do not require (accurate) knowledge of the friction characteristic. This inherently induces a certain level of robustness for uncertain friction or changing operating conditions, but these control architectures exhibit certain characteristic drawbacks. PID control of motion systems subject to friction with the Stribeck effect may lead to hunting limit cycling, see e.g., Armstrong-Hélouvry et al. [1994], Hensen et al. [2003]. Integrator action allows the system to escape the stick phase, since it eventually compensates for the static friction. However, due to the velocity-weakening Stribeck effect, the friction is overcompensated in the slip phase, which results in in a stick-slip oscillation around the set-point. Dithering-based approaches (see e.g., Armstrong-Hélouvry et al. [1994], Thomsen [1999]) use high-frequent vibrations to smoothen the discontinuity induced by the friction, thereby risking the excitation of high-frequency system dynamics. The

⋆ This research is supported by the Dutch Technology Foundation (STW, project 13896).

10.1016/j.ifacol.2017.08.661

same drawback holds for impulsive control (see e.g., van de Wouw and Leine [2012]), where impulsive control signals are employed when the system 'sticks' at a non-zero position error, such that the system escapes such a stick phase.

In this work, we present a control technique that guarantees set-point stabilization of a motion system subject to static friction and the Stribeck effect. The proposed control architecture will be shown to be robust for unknown, possibly slowly time-varying, static friction and an uncertain Stribeck effect. The controller consists of a switching PID controller, combined with an auxiliary control term that robustly compensates the Stribeck effect, thereby eliminating hunting limit cycling and guaranteeing asymptotic set-point stability.

This article is organized as follows. In Section 2, the considered control problem is specified and Section 3 covers the controller design. Next, a stability analysis is presented in Section 4. The effectiveness of the presented controller is illustrated by means of a numerical example in Section 5. A conclusion is presented in Section 6.

2. CONTROL PROBLEM FORMULATION

Consider a motion system consisting of an inertia m, subject to static friction including the velocity-weakening effect, as schematically visualized in Fig. 1. The system is described by the dynamics

$$\dot{x}_1(t) = x_2(t), \tag{1a}$$

$$\dot{x}_2(t) = \frac{1}{m}\left(F_f - u(t)\right). \tag{1b}$$

The position of the inertia is denoted by x_1, its velocity by x_2, and the control input is denoted by u. We assume that the set-point is the origin, i.e., $x_1 = x_2 = 0$. The friction force is represented by F_f, which consists of a set-valued Coulomb friction contribution with an uncertain static friction F_s, and a smooth, velocity-dependent contribution $f(x_2)$, inducing a velocity-weakening effect, see Fig. 2, i.e.,

$$F_f \in -F_s\mathrm{Sign}(x_2) + f(x_2), \tag{2}$$

where the *set-valued* sign function is defined as

$$\mathrm{Sign}(y) := \begin{cases} -1, & y < 0 \\ [-1,\ 1], & y = 0 \\ 1, & y > 0 \end{cases}, \tag{3}$$

written with a capital S. The *classical* sign function is defined as

$$\mathrm{sign}(y) := \begin{cases} -1, & y < 0 \\ 0, & y = 0 \\ 1, & y > 0 \end{cases}, \tag{4}$$

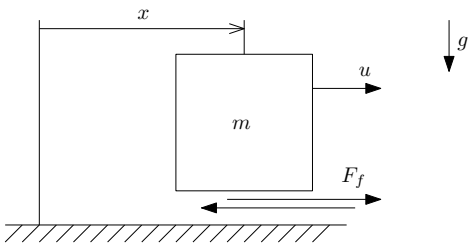

Fig. 1. Schematic representation of the motion system subject to friction.

written with a lower-case s, which will also be used in the controller later on. The model in (1), (2) together constitutes a differential inclusion. The smooth part of the friction $f(x_2)$ is also considered to be potentially uncertain. The only assumption adopted for f is that it satisfies the inequality

$$x_2 f(x_2) \leq -|x_2|\tilde{F}\left(e^{-\delta|x_2|} - 1\right), \tag{5}$$

for all $x_2 \in \mathbb{R}$. Herein, $\tilde{F} \in \mathbb{R}_{>0}$ is chosen such that the magnitude of the velocity-dependent friction part is bounded by $\tilde{F}$, as visualized in the right subplot of Fig. 2. Although alternative ways of defining a bound on the velocity-dependent curve may exist, the benefit of the inequality (5) is the fact that it is characterized by only two parameters, namely $\tilde{F}$, and a parameter $\delta \in \mathbb{R}_{>0}$, which embeds a velocity-dependency in this bound, while still allowing to characterize the Stribeck (velocity-weakening) effect commonly present in frictional contact.

Remark 1. Although not explicitly taken into account here, viscous friction can also be added to the friction model in (2) and the developments of this paper will still be valid.

Remark 2. Due to changing operating conditions, the friction characteristic may vary over time. The controller presented in this paper is robust for quasi-constant friction, i.e., the static friction F_s and the velocity-dependent contribution $f(x_2)$ may be time-varying, but only on a slower time scale than that of the closed-loop dynamics.

Let us now pose the following assumptions on the control system and the bound on the smooth part of the friction (5).

Assumption 1. Prior to activation of the controller presented in this article, the system is regulated by a PD controller to the corresponding stick set, see e.g., Putra et al. [2007]. A PD-controlled inertia subject to friction as described by (1), (2) exhibits an equilibrium (stick) set given by $\mathcal{E}_s := \{|x_1| \leq F_s/K_p,\ x_2 = 0\}$, where $K_p \in \mathbb{R}_{>0}$ represents the proportional gain of this PD controller, and solutions typically converge to this equilibrium set in finite time. Therefore, the initial conditions for our control problem are assumed to satisfy $[x_1(0),\ x_2(0)]^\top \in \mathcal{E}_s$.

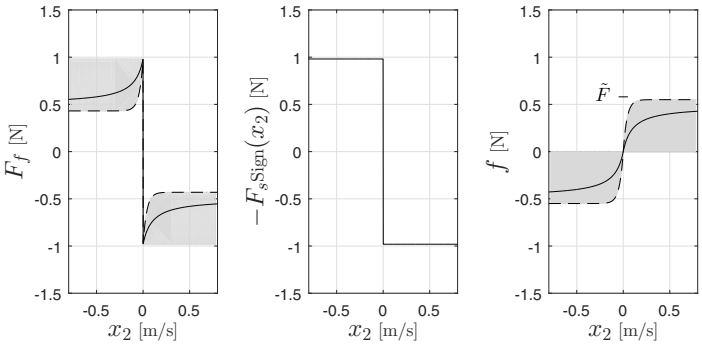

Fig. 2. An example of a friction characteristic (left) that can be decomposed into static friction (center) and a velocity-dependent Stribeck curve (right). The dashed line indicates the usage of the bound (5).

Assumption 2. It is assumed that, firstly, the bound in (5) holds and, secondly, that $0 < \tilde{F} \leq F_s$, such that the bound on the total friction characteristic

$$\left| -F_s \text{Sign}(x_2) - \tilde{F}\left(e^{-\delta|x_2|} - 1\right) \text{sign}(x_2) \right| \geq 0, \quad (6)$$

represents a friction characteristic that does not induce negative damping [1], see the dashed line in the left subplot of Fig. 2.

The control problem considered in this paper is stated as follows.

Problem 1. Design a control law for u of system (1), such that, given Assumptions 1-2, the set-point $[x_1,\ x_2]^\top = [0,\ 0]^\top$ is asymptotically stabilized.

3. CONTROLLER DESIGN

In order to solve Problem 1, a controller that consists of a switched PID term v, and a term w that robustly compensates for velocity-dependent and uncertain frictional effects (including the Stribeck effect), is employed. Integrator action plays an important role, as it is required to compensate for the uncertain static friction such that the system can escape the stick phase. The switching dynamic control law is given by

$$\dot{x}_3 = \begin{cases} |x_1|, & \text{if } t < t_1 \vee (t \geq t_1 \wedge x_3 < \bar{x}_3), \\ 0, & \text{if } t \geq t_1 \wedge x_3 = \bar{x}_3, \end{cases} \quad (7a)$$

$$v = K_p x_1 + K_d x_2 - K_i x_3 \left(\text{sign}(x_2) - (1 - |\text{sign}(x_2)|)\,\text{sign}(x_1)\right), \quad (7b)$$

$$w = -\tilde{F}\left(e^{-\delta|x_2|} - 1\right)\text{sign}(x_2), \quad (7c)$$

$$u = v + w, \quad (7d)$$

where

$$\bar{x}_3 = x_3(t_1) + \frac{K_p|x_1(t_1)|}{K_i}, \quad (7e)$$

$$t_1 := \max\{t \in \mathbb{R}_{\geq 0} \mid x_2(s) = 0 \wedge \dot{x}_2(s) = 0,\ \forall s \in [0, t]\}, \quad (7f)$$

with initial condition $x_3(0) = 0$. The proportional, derivative, and integral control gains of the PID controller in (7b) are denoted by K_p, K_d, $K_i \in \mathbb{R}_{>0}$, respectively (the proportional and derivative control gains should be tuned such that the transient performance for $t < 0$ is acceptable, see Assumption 1). The integrator dynamics (7a) result in a *saturated* integrator state $x_3 \in \mathbb{R}_{\geq 0}$, which cannot exceed a maximum value defined by $\bar{x}_3$, such that it only compensates for the static friction. Its value is determined at the first stick-slip transition of the system, at $t = t_1$, see (7f). Note that the integrator takes an anti-windup-like design w.r.t. the static friction, and that the case logic in (7a) is partially time-dependent, since $\bar{x}_3$ is undefined for $t < t_1$. Moreover, in this particular design of the integrator the *absolute value* of the position error is integrated over time and thus $x_3 \geq 0$ holds for all $t \geq 0$. The switching term $\text{sign}(x_2) - (1 - |\text{sign}(x_2)|)\,\text{sign}(x_1)$ in (7b) is then employed to determine the sign of the integrator control force. If $x_2 \neq 0$, the sign of the velocity x_2 determines the sign of the integrator control force, whereas the sign of the position error x_1 determines the sign of the force for $x_2 = 0$. In this way, the contribution of integrator action is still present when the system is in the stick phase ($x_2 = 0$). A conventional PID controller, where the position error is integrated over time (not its absolute value), does not employ such a term. If overshooting the set-point occurs, the conventional integrator state has to change sign by gradually depleting and refilling its buffer in order to provide integral action in the correct direction. This process is slow, and leads to large settling times. The proposed controller, instead, leads to considerably faster convergence when overshoot of the set-point occurs, by using switching controls. This particular design also supports set-point stability, as we will explain in the next section.

[1] Note that in (6), both the set-valued as the classical sign functions appear, as defined in (3) and (4), respectively.

4. STABILITY ANALYSIS

In this section, we show that the controller presented in the previous section asymptotically stabilizes the set-point $[x_1,\ x_2]^\top = [0,\ 0]^\top$, i.e., it provides a solution to Problem 1. To this end, we present the following theorem. Note that the initial condition $x_3(0) = 0$ represents a controller reset and is required to cope with varying static friction between subsequent set-point operations.

Theorem 1. *Consider the closed-loop system* (1), (2), (7), *with initial conditions* $0 < |x_1(0)| \leq F_s/K_p$, $x_2(0) = x_3(0) = 0$, *satisfying Assumption 1-2. Moreover, consider the augmented state vector* χ, *defined as*

$$\chi := [x_1,\ x_2,\ x_3]^\top \in \Theta := \mathbb{R} \times \mathbb{R} \times \mathbb{R}_{\geq 0} \subset \mathbb{R}^3. \quad (8)$$

The set $\mathcal{C}$, *given by*

$$\mathcal{C} := \left\{ \chi \in \Theta \;\middle|\; x_1 = 0,\ x_2 = 0,\ x_3 \leq \frac{F_s}{K_i} \right\},$$

is an asymptotically stable equilibrium set of the considered closed-loop system.

Proof. The proof consists of two parts. First, we will explain the role of the (saturated) integrator state x_3, as defined in (7a) and we will show that the bound $x_3 \leq F_s/K_i$ holds. We will then use this fact to show that $\mathcal{C}$ is indeed the equilibrium set of the closed-loop system. Next, we show that the set $\mathcal{C}$ is asymptotically stable, using a Lyapunov-like stability analysis and a LaSalle-type invariance argument.

Recall the definition of the integrator state x_3, as in (7a), and the definition of its saturated value $\bar{x}_3$ in (7e). At $t = 0$, the system is in the stick phase with a (non-zero) position error, see Assumption 1. Since the system is in the stick phase and $x_3(0) = 0$, the static friction level F_s exceeds the (absolute value of the) control force for $t \in [0,\ t_1)$, i.e.,

$$F_s > K_p|x_1(t)| + K_i x_3(t), \quad t \in [0,\ t_1), \quad (9)$$

with t_1 defined in (7f). Note that $x_1(t) = x_1(0)$ for $t \in [0,\ t_1)$. At $t = t_1$, a transition from the stick phase to the slip phase takes place, which means that the static friction is exactly compensated, i.e.,

$$F_s = K_p|x_1(t_1)| + K_i x_3(t_1).$$

From the above equality, the following expression for the integrator state can be derived:

$$x_3(t_1) = \frac{F_s - K_p|x_1(t_1)|}{K_i}. \tag{10}$$

Recall that $\bar{x}_3$, see (7e), is defined as

$$\bar{x}_3 = x_3(t_1) + \frac{K_p|x_1(t_1)|}{K_i} > x_3(t_1). \tag{11}$$

Substitution of (10) in (11) yields

$$\bar{x}_3 = \frac{F_s}{K_i}. \tag{12}$$

As a result, (7a) implies that

$$x_3 \leq \frac{F_s}{K_i}, \tag{13}$$

i.e., boundedness of the integrator state x_3. Note that $x_3 = \bar{x}_3$ results in exact compensation of the static friction.

Let us now show that $\mathcal{C}$ is the equilibrium set of the closed-loop system (1), (2), (7). For $x_3 < \bar{x}_3$, it follows directly from (1), (2), (7) that $x_1 = x_2 = 0$ and thus $\mathcal{C}$ is the equilibrium set. For $x_3 = \bar{x}_3$, this is not immediately evident. In equilibrium, $x_2 = 0$ (see (1b)) then implies

$$K_p x_1 \in -F_s\text{Sign}(0) - K_i\bar{x}_3\text{sign}(x_1). \tag{14}$$

Substitution of (12) in (14) yields

$$K_p x_1 \in -F_s\text{Sign}(0) - F_s\text{sign}(x_1), \tag{15}$$

which only holds true if $x_1 = 0$, i.e., $0 \in -F_s\text{Sign}(0)$. Illustratively, for $x_1 \neq 0$ it holds true that

$$K_p x_1 \notin -F_s\text{Sign}(0) - F_s\text{sign}(x_1), \quad \text{for } x_1 \neq 0,$$

and thus $\mathcal{C}$ is the equilibrium set of the closed-loop system.

We now proceed with step 2 of the proof. Since solutions can only exist for $x_3 \leq \bar{x}_3$, it remains to show that x_1 and x_2 asymptotically tend to zero. To this end, consider the following positive semi-definite function $V : \mathbb{R}^2 \to \mathbb{R}$.

$$V(x_1, x_2) = \frac{1}{2}K_p x_1^2 + \frac{1}{2}m x_2^2.$$

The time-derivative of V satisfies

$$\begin{aligned}\dot{V} \in\ & K_p x_1 x_2 - x_2 F_s\text{Sign}(x_2) + x_2 f(x_2) - K_p x_1 x_2 \\ & - K_d x_2^2 + K_i x_2 x_3 \left(\text{sign}(x_2) - (1 - |\text{sign}(x_2)|)\text{sign}(x_1)\right) \\ & + x_2\tilde{F}\left(e^{-\delta|x_2|} - 1\right)\text{sign}(x_2).\end{aligned} \tag{16}$$

By application of (5), we obtain, after further simplifying (16):

$$\dot{V} \leq -x_2\left(F_s\text{Sign}(x_2) - K_i x_3\text{sign}(x_2)\right) - K_d x_2^2.$$

It is clear that $\dot{V} = 0$ for $x_2 = 0$. For $x_2 \neq 0$, using (13), it is concluded that $x_2\left(F_s\text{Sign}(x_2) - K_i x_3\text{sign}(x_2)\right) \geq 0$. Consequently,

$$\dot{V} \leq -K_d x_2^2, \quad x_2 \neq 0.$$

Together with $\dot{V} = 0$ for $x_2 = 0$, this implies stability of the set $\mathcal{C}$, but not yet asymptotic stability.

Next, we will use a LaSalle argument for non-smooth systems (Shevitz and Paden [1994]) to prove asymptotic stability of the set $\mathcal{C}$. In particular, we will show that $\dot{V} = 0$ *can* occur for $x_1 \neq 0$, but that $\dot{V} = 0$ can only *remain* true for $x_1 = 0$.

Consider the set

$$\mathcal{E}_0 := \{\chi \in \Theta \mid \dot{V} = 0\} = \{\chi \in \Theta \mid x_2 = 0\}.$$

According to LaSalle's Invariance princple, every solution starting in Θ converges to the largest invariant set $\mathcal{E}_M \subset \mathcal{E}_0$ for $t \to \infty$ (Shevitz and Paden [1994]). Let $[x_1(t),\ x_2(t),\ x_3(t)]^\top$ be a solution of the closed-loop system (1), (2), (7) that belongs identically to $\mathcal{E}_0$, i.e., $x_2 \equiv 0 \Rightarrow \dot{x}_2 \equiv 0$, which, in turn, implies

$$0 \in -F_s\text{Sign}(0) - K_p x_1 - K_i x_3\text{sign}(x_1). \tag{17}$$

In order to find the set $\mathcal{E}_M$, the values of x_1 for which (17) holds true must be determined. To this end, we will consider the cases $x_1 = 0$, $x_1 > 0$, and $x_1 < 0$ separately, to determine whether or not (17) holds.

Case 1: $x_1 = 0$

For $x_1 = 0$, (17) holds since indeed $0 \in -F_s\text{Sign}(0)$.

Case 2: $x_1 > 0$

For $x_1 > 0$ and $x_2 = 0$, the algebraic inclusion in (17) can be expressed as the following two inequalities:

$$K_p x_1 + K_i x_3 \geq -F_s, \tag{18a}$$

$$K_p x_1 + K_i x_3 \leq F_s. \tag{18b}$$

If both inequalities hold for any $x_1 > 0$, then (17) holds as well for that $x_1 > 0$. Inequality (18a) holds true for all values of x_3, since $x_3 \geq 0$ and $x_1 > 0$. Inequality (18b), however, only holds true for $x_3 \leq \frac{F_s - K_p x_1}{K_i}$. Since the system is in stick ($x_2 = 0$) with a positive, non-zero position error, i.e., $x_1 > 0$, we have $x_3 < \bar{x}_3$ and, consequently, $\dot{x}_3 = |x_1|$ (see (7a)). As a result, the integrator state x_3 will keep increasing such that eventually $x_3 > \frac{F_s - K_p x_1}{K_i}$. At this point, the control force has exceeded the static friction such that the system is no longer in the stick phase. As a result, (18b), and thus (17), cannot remain true for any $x_1 > 0$.

Case 3: $x_1 < 0$

For the case $x_1 < 0$ and $x_2 = 0$, a similar reasoning to Case 2 holds.

From the above analysis, we conclude that the largest invariant set in $\mathcal{E}_0$ is given by

$$\mathcal{E}_M = \left\{\chi \in \Theta \mid x_1 = 0,\ x_2 = 0,\ x_3 \leq \frac{F_s}{K_i}\right\},$$

and thus the set $\mathcal{C}$ is attractive and asymptotically stable. This concludes the proof for Theorem 1. ■

Remark 3. We care to stress that Theorem 1 guarantees asymptotic stability of the set $\mathcal{C}$ (for which $x_1 = x_2 = 0$) for a whole range of friction characteristics. For the velocity-dependent part of the friction, it can be concluded that for any friction law that lies in the grey area in Fig. 2, stability is guaranteed. In this figure, the actual and model values of the static friction level F_s match (for the sake of illustration). However, the control algorithm guarantees robust stability for any bounded static friction level as long as the inequality in (6) is satisfied, which in fact, given a choice for $\tilde{F}$, expresses a lower bound for F_s.

5. ILLUSTRATIVE EXAMPLE

In this section, the working principle and effectiveness of the presented control architecture are illustrated by means of an example. To this end, consider the motion system of Fig. 1, described by the closed-loop dynamics (1), (2), (7),

with parameter values $m = 1$ kg, $g = 9.81$ m/s^2, $K_p = 18$, $K_d = 1$, and either $K_i = 10$, $K_i = 20$ or $K_i = 30$. The *true* friction characteristic, given by (2), satisfies $F_s = \mu mg$, with $\mu = 0.1$ the friction coefficient. The true Stribeck curve is assumed to satisfy

$$f(x_2) = ((\mu mg - F)\eta x_2)\,(1 + \eta|x_2|)^{-1}, \qquad (19)$$

with $F = 0.5$ N the true dynamic friction, and $\eta = 20$ the Stribeck shape parameter. This results in the particular friction characteristic visualized in Fig. 2, with a pronounced Stribeck effect. The bound on the Stribeck curve satisfies (5), with $\delta = 25$ and $\tilde{F} = 0.55$ N, which results in the particular bound as presented in Fig. 2.

A numerical time-stepping routine (see Acary and Brogliato [2008]) is employed to numerically compute solutions of the closed-loop system. The initial conditions are $x_1(0) = -0.05$, $x_2(0) = x_3(0) = 0$, satisfying Assumption 1. The response of the closed-loop system is visualized in Fig. 3, for both $K_i = 10$, $K_i = 20$, and $K_i = 30$, to illustrate the influence of the integral gain K_i on the transient response.

For $K_i = 10$, the response approaches the set-point $x_1 = 0$ asymptotically without overshoot, and with the only period of sticking occurring immediately after $t = 0$. The integrator state x_3 approaches $\bar{x}_3 = F_s/K_i$ asymptotically, thereby effectively compensating for the unknown static friction. The corresponding control forces v and w are presented in Fig. 4. The total control signal $v + w$ is smooth, such that excitation of high-frequency system dynamics is prevented due to the absence of discontinuous control signals.

For $K_i = 20$, the response converges faster to the set-point $x_1 = 0$ compared to the response with $K_i = 10$, but now with intermediate periods of stick (i.e., $x_2 = 0$), see the zoomed box in the middle subplot of Fig. 3. This is consistent with the LaSalle argument discussed in the previous section, as the response may arrive in the stick phase with a non-zero position error, but it cannot remain there due to the integrator action. The corresponding control force, see Fig. 4, is continuous but non-smooth, due to the non-smooth contribution of w caused by the sticking instants.

For $K_i = 30$, the response overshoots the set-point $x_1 = 0$, but still converges to the set-point (in compliance with Theorem 1). This integrator tuning results in a saturated integrator state (i.e, $x_3 = \bar{x}_3$), see the zoomed box in the lower subplot of Fig. 3, and a discontinuous control signal v, as can be seen in Fig. 5. Since the discontinuity in the integrator control force occurs only at velocity reversals, there will be no excitation of high-frequency system dynamics, as illustrated by the following reasoning. It holds that $x_3 \leq F_s/K_i$, so the integrator action compensates (partially) for the static friction. The static friction changes sign upon velocity reversal, and so does the integrator action. If $x_3 = F_s/K_i$ at a velocity reversal, the integrator control force and static friction cancel each other such that the remaining dynamics consist of merely a PD-controlled inertia. Fig. 6 illustrates that the net force acting on the inertia is a smooth function of time. If the system overshoots the set-point with a small amplitude while still $x_3 < F_s/K_i$, the system may arrive in the stick phase again since the integrator control force (combined with a low proportional control force due to a small position error) may not fully compensate for the static friction. Then, the integrator force changes sign at zero velocity, but the total control force may not be sufficient for the system to escape the stick set and thus

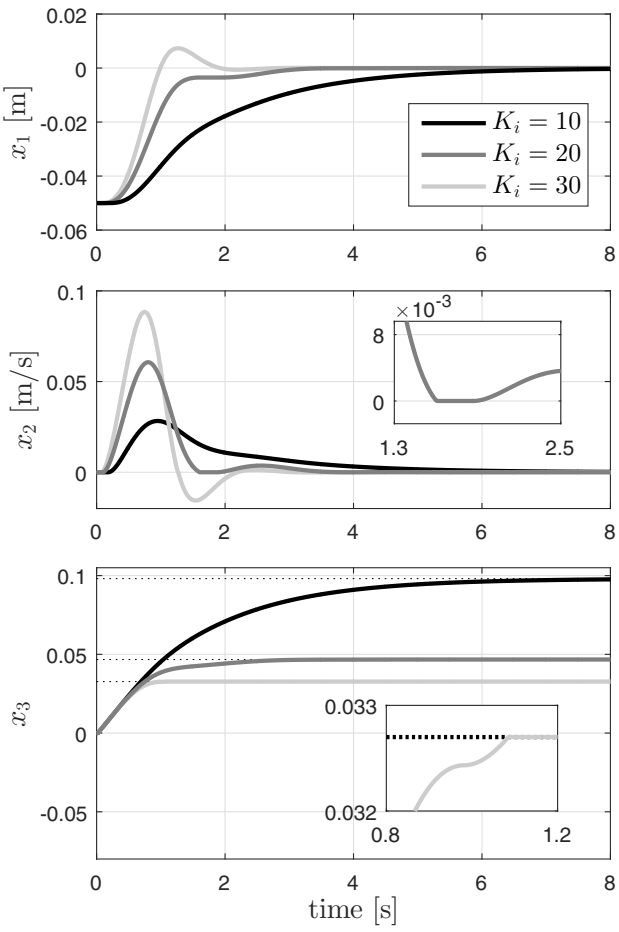

Fig. 3. Simulated response of the closed-loop system. Time history of the position (top), velocity (middle) and integrator state (bottom). The dotted black lines in the bottom subplot indicate the corresponding value for $\bar{x}_3 = F_s/K_i$.

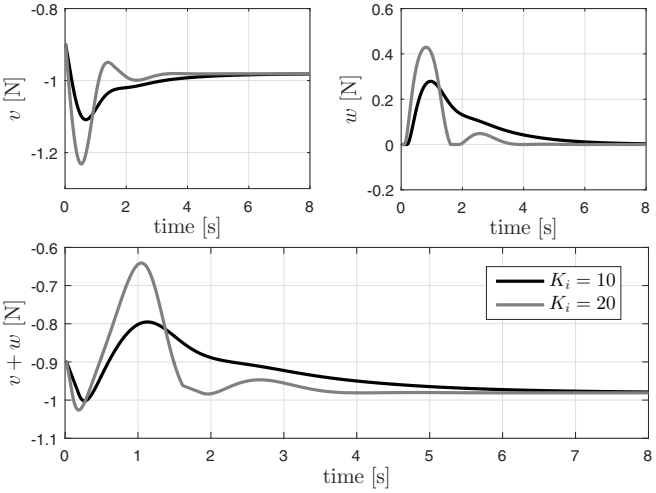

Fig. 4. Control forces for $K_i = 10$ and $K_i = 20$.

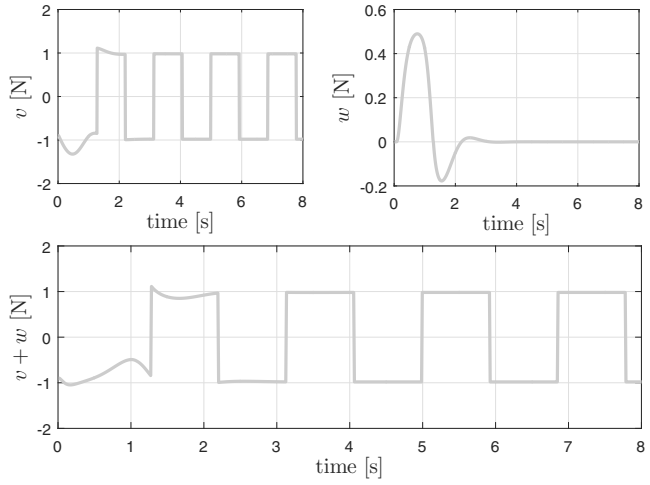

Fig. 5. Control forces for $K_i = 30$.

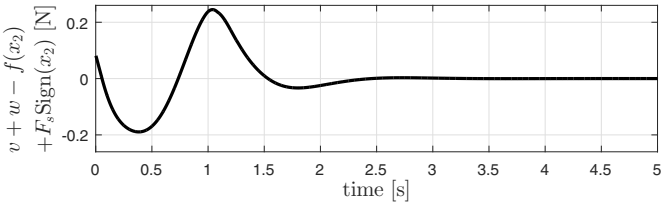

Fig. 6. Net force acting on the inertia during simulation with $K_i = 30$.

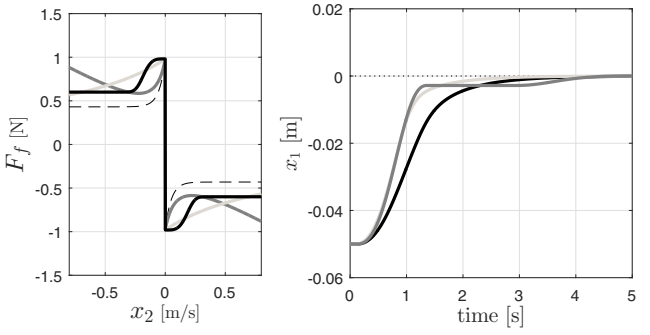

Fig. 7. Simulated response of the closed-loop system for variations on the velocity-dependent contribution of the friction. The dashed line indicates the usage of the bound (5) on this contribution.

the discontinuity in the control force does not result in motion of the system.

By design of the controller (7), every velocity-dependent friction law that satisfies (5), i.e., that lies inside the grey area in Fig. 2 results in asymptotic set-point stability. The simulated responses of the closed-loop system (1), (2), (7) (with the same parameter settings and $K_i = 20$) for different velocity-dependent friction curves illustrate this fact, see Fig. 7.

6. CONCLUSIONS

In this paper, a control architecture for the set-point stabilization of motion systems subject to set-valued Stribeck friction is proposed. The controller consists of a switching PID term, and a term that robustly compensates for the velocity-weakening contribution of the friction. The controller is robust for both unknown static friction, and an uncertain Stribeck curve. The control strategy guarantees asymptotic convergence to the set-point, and the particular design of the integrator action allows for considerable faster convergence if the trajectory overshoots the set-point, compared to the usage of conventional integrator action in (7b). The effectiveness of the control architecture is illustrated by means of a motion control example.

REFERENCES

Acary, V. and Brogliato, B. (2008). *Numerical Methods for Nonsmooth Dynamical Systems*, volume 35.

Amthor, A., Zschaeck, S., and Ament, C. (2010). High precision position control using an adaptive friction compensation approach. *IEEE Trans. on Autom. Control*, 55(1), 274–278.

Armstrong-Hélouvry, B., Dupont, P., and Canudas de Wit, C. (1994). A survey of models, analysis tools and compensation methods for the control of machines with friction. *Automatica*, 30(7), 1083–1138.

Freidovich, L., Robertsson, A., Shiriaev, A., and Johansson, R. (2010). LuGre-model-based friction compensation. *IEEE Trans. Control Syst. Technol.*, 18(1), 194–200.

Hensen, R., Van de Molengraft, M., and Steinbuch, M. (2003). Friction induced hunting limit cycles: A comparison between the LuGre and switch friction model. *Automatica*, 39(12), 2131–2137.

Makkar, C., Hu, G., Sawyer, W.G., and Dixon, W.E. (2007). Lyapunov-based tracking control in the presence of uncertain nonlinear parameterizable friction. *IEEE Trans. Autom. Control*, 52(10), 1988–1994.

Márton, L. and Lantos, B. (2009). Control of mechanical systems with Stribeck friction and backlash. *Systems & Control Letters*, 58(2), 141–147.

Na, J., Chen, Q., Ren, X., and Guo, Y. (2014). Adaptive prescribed performance motion control of servo mechanisms with friction compensation. *IEEE Trans. Ind. Electronics*, 61(1), 486–494.

Olsson, H. and Astrom, K. (1996). Observer-based friction compensation. *Proc. 1996 IEEE Conference on Decision and Control*, 4345–4350.

Panteley, E., Ortega, R., and Gäfvert, M. (1998). An adaptive friction compensator for global tracking in robot manipulators. *Systems & Control Letters*, 33(5), 307–313.

Putra, D., Nijmeijer, H., and van de Wouw, N. (2007). Analysis of undercompensation and overcompensation of friction in 1DOF mechanical systems. *Automatica*, 43(8), 1387–1394.

Rijlaarsdam, D., Nuij, P., Schoukens, J., and Steinbuch, M. (2012). Frequency domain based nonlinear feed forward control design for friction compensation. *Mechanical Systems and Signal Processing*, 27(1), 551–562.

Shevitz, D. and Paden, B. (1994). Lyapunov Stability Theory of Nonsmooth Systems. *IEEE Trans. Autom. Control*, 39(9), 1910–1914.

Thomsen, J. (1999). Using fast vibrations to quench friction-induced oscillations. *Journal of Sound and Vibration*, 228(5), 1079–1102.

van de Wouw, N. and Leine, R. (2012). Robust impulsive control of motion systems with uncertain friction. *Int. J. Robust and Nonlinear Control*, 22, 369–397.